Analysis of the Frequency and Power Performances of Tunnel Diode Generators*

H. J. OGUEY†, MEMBER, IEEE

Summary—This analysis shows the order of magnitude of the highest frequency and power to be expected from a single tunnel diode generator. An optimization on the circuit level indicates how to make the best use of a given device. The influence of the dimensions and the geometry is considered and relates the performances of the circuit with bulk and junction properties of the semiconductor. On the basis of empirical data, a correlation between bulk and junction properties is established and relates all of them to the doping level and the basic semiconductor used. Numerical data show the physical limitations to be expected with germanium and gallium-arsenide in relation with two idealized cavity geometries. As dimensions cannot be arbitrarily reduced, nor the impedance be arbitrarily low, they introduce other limitations which prevent in some cases the possibility of optimum performances and show comparable merits of the two geometries. It is concluded that a power output of 5 mw at 30 kMc for a GaAs tunnel diode generator is an optimistic figure close to the technical limit.

I. Introduction

SHORTLY AFTER the discovery of the tunnel diode by Esaki [1], it was realized that one of the important applications of this two-terminal device would be the generation of high-frequency oscillation [2]. More recently, many authors have reported successful operation in the kMc range. Some of the highest powers obtained so far (as of April, 1962) are summarized in Table I.

As time goes on, it is likely that these figures will be improved and the questions naturally arising are 1) what limitations of theoretical nature do exist, and 2) according to these limitations, what the geometries and materials permit reaching the highest powers and frequencies? The present report is an attempt to answer these questions, and especially to widen the scope of previous studies [4], [7] by including geometry and material considerations.

TABLE I

Highest Power Output Reported in the Literature for Single Tunnel Diode Generators

Frequency f (kMc)	Power P (μw)	fP (Mc×w)	I_p (ma)	Wafer Material	Reference
2.8	700	1.96	37	Ge	[3]
10.0	200	2.0	2.0	Ge	[4]
1.6	15,000	24	200	GaAs	[4]
6.0	4,000	24		GaAs	[5]
17	50	0.85	3	p–GaAs	[6]
50	25	1.25	3.5	n–GaAs	[6]
90	2	0.18	1.8	n–GaAs	[6]

* Received February 12, 1963; revised manuscript received April 29, 1963.

† IBM Research Laboratory, Ruschlikon ZH, Switzerland. Formerly with IBM Thomas J. Watson Research Center, Yorktown Heights, N. Y.

The following assumptions are made throughout this study:

1) The distributed parameter aspect of oscillators can be approximated by lumped frequency-independent parameters up to the highest frequencies. Skin effect is neglected. Multimode operation is not considered.
2) Except for the junction voltage-current characteristics, all other elements are assumed linear. The voltage-dependence of the junction capacitance is neglected.
3) The junction voltage-current characteristics are assumed to be instantaneous (no delay effect due to finite tunneling time, indirect transitions, or minority carrier storage) and is represented in a unified way by a cubic characteristic matching the experimental curve at the peak and valley points.
4) The device works at room temperature.

II. Circuit Analysis and Optimization

Two circuits will be considered in this article, the parallel circuit and the series-parallel circuit. In both, the tunnel diode will be decomposed in a nonlinear element with instantaneous current-voltage characteristics and in linear lumped elements. The load and the losses in bulk material will be represented by linear resistances, and the resonant circuit by a linear LC combination.

A. The Parallel Circuit

The parallel circuit (Fig. 1) is the simplest tunnel diode oscillator circuit. It consists of a linear inductance L_p, a linear capacitance C, a linear load conductance G_p, and a nonlinear element N assumed to have a frequency-independent characteristic $I_n(V)$ in series with a dc voltage source E. Such a circuit can be realized with a good approximation at low and medium frequencies, as long as the reactive parameters of the tunnel diode can be neglected. The nonlinear $I_n(V)$ characteristics of a tunnel diode need a large number of parameters in order to be defined accurately. It has been shown elsewhere [8] that once the peak and valley points have been defined, the maximum power and the frequency are not much affected by local changes of the shape. Consequently, in an analysis such as this one, where orders of magnitude only are of interest, the simplest possible mathematical expression will be used to represent the characteristics, namely a cubic curve, the extrema of which are the peak and the valley (Fig. 2). The advantage of a continuous approximation,

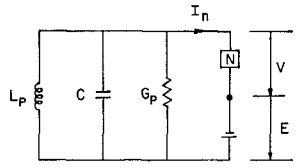

Fig. 1—Parallel tunnel diode circuit.

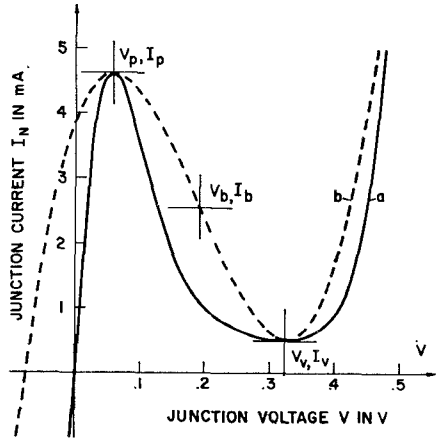

Fig. 2—(a) Tunnel diode experimental characteristics (Ge); (b) Cubic approximation having same peak (V_p, I_p) and valley (V_v, I_v) points. The cubic approximation is antisymmetrical with respect to the bias point (V_b, I_b).

compared to a limited linear characteristic, as assumed, for example, by Dermit [7], is that the amplitude of oscillation is not assumed *a priori*, but evolves as the stable periodic solution of the system equation.

The voltage and current V and I_n in Fig. 1 are the superposition of the variable voltage and current v and i and of the bias voltage and current V_b and I_b assumed to be in the middle between peak and valley. The nonlinear characteristic is:

$$i = G_1 v + G_3 v^3. \tag{1}$$

The coefficients G_1 and G_3 are chosen for coincidence of peak and valley points between analytical and experimental characteristics:

$$G_1 = -\frac{3}{2}\frac{I_p - I_v}{V_v - V_p} < 0; \quad G_3 = 2\frac{I_p - I_v}{(V_v - V_p)^3} > 0. \tag{2}$$

G_1 is the slope of the analytical characteristics at the bias point. The slope of an experimental characteristic generally has a higher absolute value in its steepest part.

The differential equation representing the system has been derived by many authors who followed essentially the same way as did van der Pol for triode oscillators [9]:

$$L_p C\frac{d^2v}{dt^2} + L_p\left(\frac{di}{dt} + G_p\frac{dv}{dt}\right) + v = 0. \tag{3}$$

Now (1) is introduced into (3) and the change of variables is made:

$$t = \tau\sqrt{L_p C}; \qquad v = x\sqrt{\frac{-(G_1 + G_p)}{3G_3}}. \tag{4}$$

Eq. (3) reduces to the van der Pol equation

$$\frac{d^2x}{d\tau^2} - \lambda(1 - x^2)\frac{dx}{d\tau} + x = 0, \tag{5}$$

where

$$\lambda = -(G_1 + G_p)\sqrt{\frac{L_p}{C}}. \tag{6}$$

This equation has been intensively investigated in the literature. It is known [10] that a stable limit cycle or stable periodic solution exists for all positive values of λ. This solution is reached asymptotically for every initial condition. For small values of λ, the periodic solution is nearly sinusoidal and its period is 2π. For large values of λ, the periodic solution is of the relaxation type and its period is nearly proportional to λ.

In the following, emphasis will be given on the harmonic solutions corresponding to low values of λ. The following approximate values of the oscillation amplitude $\hat{x}$ and of the angular frequency Ω will be used [10], [11]:

$$\hat{x} = 2; \qquad \Omega = 1. \tag{7}$$

The amplitude expression is accurate to within 1.5 per cent in the entire range of value of λ as can be compared with direct calculations [12]. Ω is correct within 2 per cent [12] for

$$\lambda \leq 0.57. \tag{8}$$

Van der Pol [9] showed a direct relation between frequency Ω and harmonic content of the voltage, whereby a low harmonic content always calls for a small deviation of Ω with respect to 1. For this reason, the case $\lambda = 0.57$ will be called harmonic limit. From (2), (4) and (7), the mean ac power into the conductance G_p is

$$P_{ac} = \tfrac{3}{4}(V_v - V_p)(I_p - I_v)k(1 - k) \tag{9}$$

with the matching coefficient

$$k = -G_p/G_1. \tag{10}$$

B. The Series-Parallel Circuit

In the series-parallel circuit, the resistance is in series with the inductance. This circuit is useful in determining the frequency limit of a tunnel diode oscillator, where the only capacitance is the junction capacitance, C_j, and where the bulk material resistance is represented by R_D (Fig. 3). The load resistance R_L and the series inductance L_s have to be chosen such that a high power output is obtained at high frequency.

Strictly speaking, the circuit of Fig. 3 cannot be reduced to a parallel circuit (Fig. 1) nor can it be expressed by the van der Pol equation (5). But under the assumption of a nearly sinusoidal periodic solution (a fairly low value of λ), a series-parallel transformation can be used, which is accurate for the basic angular frequency ω of

the oscillation. Within the range of validity of (7) we get

$$L_p = L_s\left[1 + \left(\frac{R_L + R_D}{\omega L_s}\right)^2\right]$$

$$\cong \frac{L_s^2}{L_s - (R_L + R_D)^2 C} \tag{11}$$

$$G_p = \frac{(R_L + R_D)}{(\omega L_s)^2 + (R_L + R_D)^2}$$

$$\cong (R_L + R_D)\frac{C}{L_s}\cdot \tag{12}$$

Recently a direct analysis of the series circuit by Miranker [13] proved the identity of the first approximation with the indirect approach taken here. A better approximation of the amplitude and of the frequency as in (7) would not give a better accuracy after the transformation. A similar observation has been made by Schuller and Gartner [14] in comparing an exact computer solution with an approximate method involving the van der Pol equation.

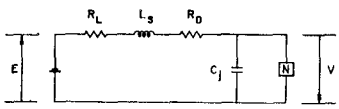

Fig. 3—Series-parallel tunnel diode circuit.

The effect of the diode series resistance R_D is to dissipate some of the ac power. The ac efficiency η is defined as the fraction of the ac power P_{ac} available to the load R_L as output power P_o. It is related to the series resistances:

$$\eta = \frac{P_o}{P_{ac}} = \frac{R_L}{R_L + R_D}\cdot \tag{13}$$

From (9) the output power is

$$P_o = \tfrac{3}{4}(V_v - V_p)(I_p - I_v)k(1 - k)\eta. \tag{14}$$

Two diode parameters are introduced here which are important for high-frequency applications: the junction time constant T and the relative diode resistance r. They are defined by

$$T = -C_j/G_1; \qquad r = -R_D G_1. \tag{15}$$

Both quantities are positive as G_1 is negative. The preceding relations for matching and frequency are related to T, r, k and η in the following way:

$$k(1 - \eta) = \frac{rT^2}{L_s C} \tag{16}$$

$$f = \frac{1}{2\pi T}\sqrt{\frac{k(1-\eta)}{r}}\sqrt{1 - \frac{kr}{1-\eta}}\cdot \tag{17}$$

The harmonic limit (8) defines the range of approximate validity of this equation. According to the dependence between f and λ, we see that the upper bound of λ sets a lower limit to the frequency:

$$= \frac{1-k}{2\pi\lambda T} > \frac{1-k}{1.14\pi T}\cdot \tag{18}$$

C. Choice of the Parameters for Optimum Performances

For a given diode the load resistance R_L and the series inductance L_s can be chosen arbitrarily in principle. The first one will affect η (13), the second one k (16). For maximum output power [15], $k = \frac{1}{2}$, $\eta = 1$ (14), an infinitely large inductance is required, the frequency is zero. For maximum frequency (17), $k = 1$, $\eta = 0$, there is no available output power, this case corresponds to the cutoff frequency [16].

In practical applications, both power and frequency should be large, and, in the following, our criterion for optimum performance will be the maximum of the power-frequency product. Assuming the second term under the square-root sign in (17) much smaller than 1, this square root, developed in a Taylor expansion, reduces to the first two terms. The optimum conditions are easily found by equating to zero the partial derivatives of the $P_o f$ product with respect to the parameters η and k. This optimum case will be designed with the index m:

$$k_m = \frac{3}{5}; \qquad \eta_m = \frac{2}{3} \tag{19}$$

$$P_{om} = 0.12(V_v - V_p)(I_p - I_v) \tag{20}$$

$$f_m = \frac{0.0712}{T\sqrt{r}}\sqrt{1 - 1.8r} \tag{21}$$

$$L_{sm} = 5\frac{rT^2}{C}\cdot \tag{22}$$

Under these conditions, the optimum power is about 64 per cent of its highest possible value, and the optimum frequency 45 per cent of the resistive cutoff frequency. The limitation on λ, in this case, leads to

$$r \leq \frac{5}{21}; \qquad f_m \geq \frac{0.11}{T}\cdot \tag{23}$$

III. Geometry, Dimensions and Intrinsic Properties

The preceding relations were limited to the case where the diode was given. If no specifications are made on the dimensions and geometry of the diode and of the oscillator, their influence on power and frequency should be investigated and the way should be defined to make the best use of given material and junction properties. The quantities of interest here are the bulk resistivity ρ, the peak current density $J_p = I_p/A$, the capacitance per unit area $\gamma = C/A$, the valley to peak current ratio $\zeta = I_v/I_p$, and the peak and valley voltages, V_p and V_v. The junction time constant is also a quantity independent of dimensions. It is related to the figure of

merit I_p/C often found in the literature:

$$T = \frac{2}{3}\frac{(V_v - V_p)\gamma}{(1-\zeta)J_p} = \frac{2}{3}\frac{(V_v - V_p)}{(1-\zeta)}\frac{C}{I_p}. \quad (24)$$

In order to give concrete figures, it is necessary to make precise assumptions about the geometry. We shall assume a cylindrical cavity of height h, outside diameter d_2, with a central column of diameter d_1 in which the pn junction is located (Fig. 4). Such an assumption seems to reduce severely the generality of this discussion, but it is felt that this geometry is fairly representative in its simplicity. On the other hand, no assumptions are made *a priori* on the dimensions, so that they can be chosen in order to provide the desired effects. Only later will limitations be considered in order to define a technical limit of feasibility. It should be noted that, in previous studies on tunnel diode oscillators, no explicit assumptions on geometry are stated, because experimental diodes are used for the numerical evaluation, so that actual diode geometry is considered as granted, and no room is left for improvements by new fabrication processes.

The cavity inductance is [17]:

$$L_s = \frac{\mu_0 h}{2\pi}\log_e\frac{d_2}{d_1}.$$

With $\mu_0 = 4\pi\times10^{-7}$ henry/meter (mks units). The order of magnitude of L_s is not much affected by large variations in the d_2/d_1 ratio. Let us assume $d_2 = 10\ d_1$. Thus we get

$$L_s \cong 0.37\mu_0 h. \quad (25)$$

Two different cases will be considered, for which the losses are concentrated in definite areas, whereas the rest of the cavity is assumed perfectly conducting [18].

A. *Case A: Cavity with Resistive Central Column*

The losses are assumed to occur here (Fig. 4) in the central column. Its resistivity ρ is assumed to be much higher than in the top and the bottom of the cavity. Consequently, the diode series resistance is

$$R_D = \frac{\rho h}{A}. \quad (26)$$

The relative diode resistance is found independent of the junction area $A = \pi d_1^2/4$

$$r = \frac{3}{2}\frac{J_p(1-\zeta)\rho h}{(V_v - V_p)}. \quad (27)$$

By elimination of L_s, a geometrical relation is found for the optimum case:

$$d_1^2 \cong \frac{10\gamma\rho(V_v - V_p)}{\mu_0 J_p(1-\zeta)}. \quad (28)$$

In the optimum case, d_1 is practically imposed by material and junction properties. The optimum output power is also determined by these factors, as can be seen easily:

$$P_{om} = 0.03\pi J_p(1-\zeta)(V_v - V_p)d_1^2 \cong \frac{\rho\gamma(V_v - V_p)^2}{\mu_0}. \quad (29)$$

The optimum frequency is given by

$$f_m = \frac{0.0616}{\gamma}\sqrt{\frac{J_p(1-\zeta)}{\rho(V_v - V_p)h}}\cdot\sqrt{1 - 2.7\frac{J_p(1-\zeta)\rho h}{V_v - V_p}}. \quad (30)$$

Neglecting the effect of the second square root, which has to be near unity for a harmonic solution, it appears that a large variation of the height h is required to produce a small variation in frequency.

B. *Case B: Cavity with Resistive Bottom*

According to some fabrication techniques, where a junction is obtained by alloying a dot of metal on a semiconductor wafer, the series resistance is likely to be distributed in the bottom of the wafer, whereas the resistance of the column and the top of the cavity can be neglected. A simple expression of the series resistance is found in the geometry of Fig. 5, where the junction

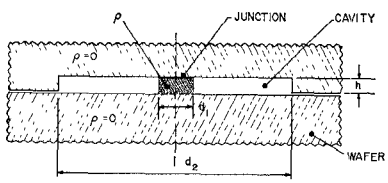

Fig. 4—Case A: Cavity with resistive central column.

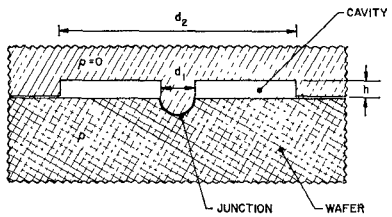

Fig. 5—Type B-geometry: Cavity with resistive bottom.

is a half sphere, and both outside diameter and thickness of the wafer are large with respect to the sphere diameter d_1 [18]

$$R_D \cong \frac{\rho}{\pi d_1}. \quad (31)$$

The junction area being $A = \pi d_1^2/2$, the relative diode resistance is now proportional to the junction diameter:

$$r = \frac{3}{4}\frac{\rho J_p(1-\zeta)d_1}{V_v - V_p}. \quad (32)$$

Optimum power and frequency are given by

$$P_{om} = 0.6\pi J_p(1-\zeta)(V_v - V_p)d_1^2 \tag{33}$$

$$f_m = \frac{0.123}{\gamma}\sqrt{\frac{J_p(1-\zeta)}{\rho(V_v - V_p)d_1}} \cdot \sqrt{1 - 1.35\frac{J_p(1-\zeta)\rho d_1}{(V_v - V_p)}} \cdot \tag{34}$$

The interesting feature in this geometry is the fact that, for a given material, power and frequency are both related to a single dimension, the junction diameter. As before, the requirement imposed on the inductance comes out as a geometrical condition:

$$d_1 h = \frac{2.8\gamma\rho(V_v - V_p)}{\mu_0 J_p(1-\zeta)} \cdot \tag{35}$$

C. Limitations

Besides the assumptions made at the beginning and the limitations already considered on λ (8), other limits of more practical character have to be considered.

The junction diameter and the cavity height are limited towards low dimensions by practical considerations. The characteristic impedance has to be higher than a minimum value in order to keep losses at a reasonable level and permit good matching to the load. The power dissipated per unit area has to be lower than a maximum permissible value. The doping level has to be kept below the value where a compound starts to be formed. These last two conditions are practically expressed by setting an upper limit to the peak current density, J_p.

IV. Material Considerations

The parameters entering (20) and (21) are functions of the semiconductor material, the doping level at both sides of the junction, the abruptness of the junction, and of some other less controllable factors. In practice, all that is known are the semiconductor materials and the doping on the wafer side of the junction. The other factors, in particular doping of the recrystallized region on the dot side, are not known and contribute to a spread of the data. For this reason, relations between ρ, γ and J_p are subject to statistical variations.

No significant correlation between peak voltage, valley voltage and valley to peak current ratio on one hand, and current density on the other hand, has been found in practice. Consequently, V_p, V_v and ζ will be assumed as functions of the semiconductor material only.

Empirical data on the relation between γ and J_p obtained from a survey of tunnel diodes made in this laboratory by different techniques are reported in Fig. 6 for Ge and GaAs [19]. An empirical curve fitting the data as well as possible is drawn and is extrapolated up to $J_p = 10^6$ A/cm^2 for Ge and up to $J_p = 10^5$ A/cm^2 for GaAs.

On the other hand, γ is related to the doping. Due to the lack of experimental data, the theoretical formula will be used, assuming the wafer has a doping concentration N much smaller than the regrown region near the dot, and assuming an abrupt junction [20].

Measurements of resistivity vs impurity concentration at room temperature have been published both for Ge [21] and GaAs [22]. All these relations have been used to compute γ, N, ρ, and T as a function of J_p for n- and p-type Ge and GaAs. The experimental values on which this computation is based as well as the results are given in Table II. Stars indicate values obtained on the basis

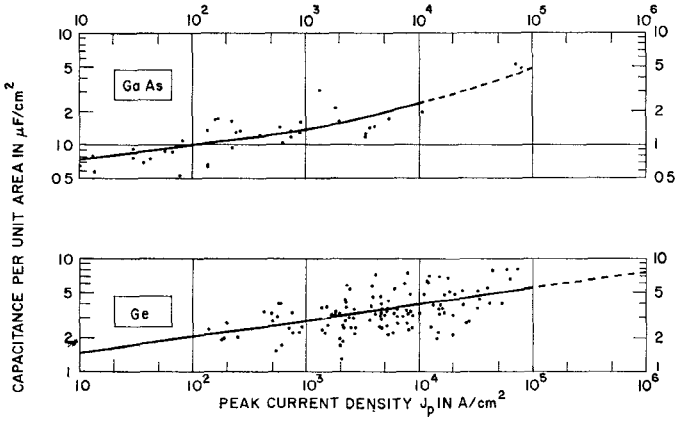

Fig. 6—Capacitance per unit area vs peak current density of experimental Ge and GaAs tunnel diodes [11].

TABLE II
Typical Tunnel Diode Parameters

Material	V_p (V)	V_v	ζ	J_p (A/cm^2)	γ (μf/cm^2)	T (ps)	$N\times10^{19}$ (cm^{-3})	$\rho\times10^4$ (Ωcm) N-doping	$\rho\times10^4$ (Ωcm) P-doping
Ge	0.07	0.32	0.12	10^3	2.85	540	1.245	14.1	22.7
				10^4	3.95	74.8	2.39	9.5	15.1
				10^5	5.45	10.3	4.55	6.5	10.1
				10^6	7.6*	1.44*	8.85*	4.4*	6.8*
Ga-As	0.15	0.55	0.08	10^3	1.35	391	0.923	4.8	70*
				10^4	2.35	68.1	2.80	2.1	30.5*
				10^5	4.7*	13.6*	11.2*	0.75*	10.6*

* Values obtained by extrapolation of empirical data.

of an extrapolation of empirical relations and are to be considered with caution. γ and T are subject to a statistical variation by a factor 2, N and ρ by a factor 4.

V. Numerical Evaluation of Tunnel Diode Generators

The preceding analysis is used to compute power and frequency graphs for Ge and GaAs. The material properties are taken from Table II, and the limitations are set to the following values:

$$d_{\min} = 10\ \mu\text{m}; \qquad h_{\min} = 10\ \mu\text{m}; \qquad Z_{\min} = 1\ \text{ohm}.$$

Current densities J_p of 10^4, 10^5 and 10^6 A/cm^2 are considered to represent respectively the actual state of the art, an upper present limit and a likely absolute technical limit. The two geometries will be considered separately.

A. Case A

Both power and frequency will be represented as a function of current density. As the junction diameter is fully determined by the required inductance (28), the optimum output power is a function of current density only. Fig. 7 shows the optimum power for n- and p-doped Ge and GaAs. An immediate conclusion of these diagrams is the lack of flexibility of this kind of geometry. The power is only slightly dependent on current density for GaAs, and almost independent of it for Ge. P-doped material gives higher power than n type, due to its higher resistivity. Large energy gap and large capacitance per unit area are further useful for large power applications. Lower powers are easily obtained by changing the matching coefficient k but higher powers are not possible without a serious drop of the frequency. Fig. 8 and Fig. 9 represent for Ge and GaAs, respectively, optimum frequency curves vs current density at the harmonic limit (23), for a constant diameter d_1, a constant height h or a constant characteristic impedance Z. Whereas a lower limit on f is set by the harmonic condition, all other limitations set upper limits to f. Furthermore, it is seen that for n and p-type Ge and for p-type GaAs, an incompatiblility exists between the harmonic and the impedance conditions defined above, so that it is not possible to get simultaneously optimum conditions for frequency-power product, harmonic operation and reasonably high characteristic

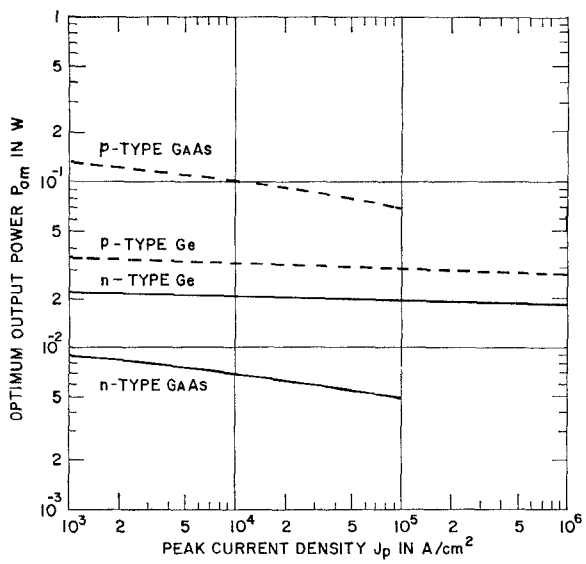

Fig. 7—Optimum output power vs peak current density for Case A, n- and p-type Ge and GaAs.

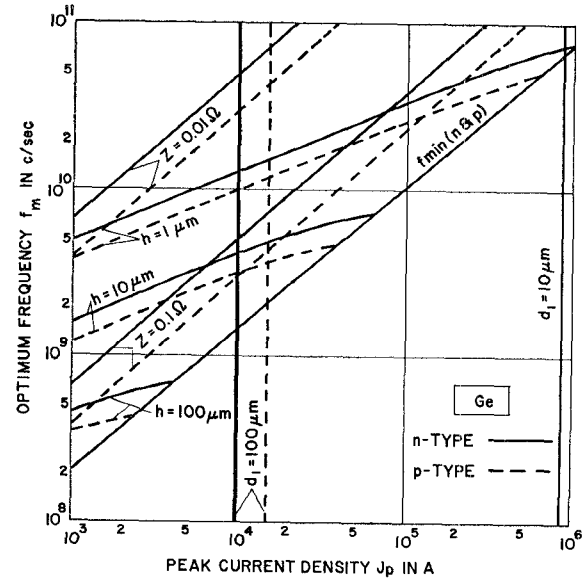

Fig. 8—Optimum frequency vs peak current density for the Case A, n- and p-type Ge, $f_{\min}$ is the harmonic limit, $Z = 0.01\ \Omega$ and $0.1\ \Omega$ are lines of constant characteristic impedance, $h = 1$, 10 and 100 μm are lines of constant cavity height, $d_1 = 10$ and 100 μm are lines of constant junction diameter.

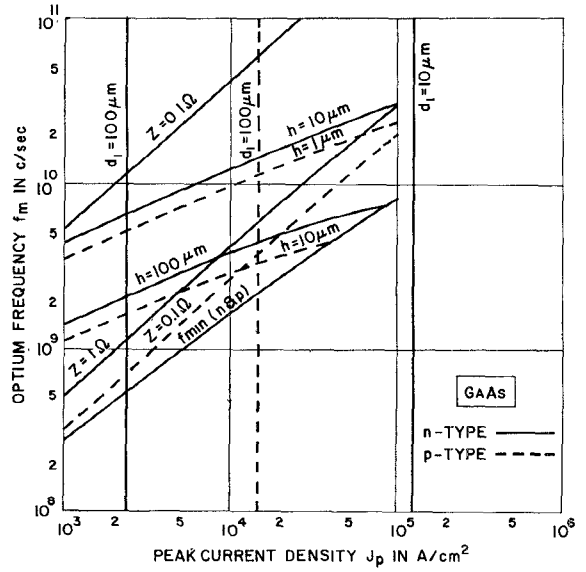

Fig. 9—Optimum frequency vs peak current density for Case A, n- and p-type GaAs. $f_{\min}$ is the harmonic limit, $Z = 1\ \Omega$ and $Z = 0.1\ \Omega$ are lines of constant characteristic impedance, $h = 1$, 10 and 100 μm are lines of constant cavity height, $d_1 = 10$ and 100 μm are lines of constant junction diameter.

impedance. Relaxation of one of the conditions means higher harmonic content and lower stability, or increased impedance matching difficulty, or lower output power. *N*-type GaAs, on the other hand, leaves a certain range of frequencies where all conditions can be met simultaneously. For example, at the limit case where the current density reaches 100,000 A/cm² and the characteristic impedance is 1 ohm, an output power of 4.9 mw is expected at a frequency of 29 kMc.

B. Case B

The fact that power and frequency are both functions of the junction diameter for a given current density permits us to draw a frequency-power diagram where current density, dimensions and characteristic impedance are represented simultaneously. Two such diagrams exist for a given semiconductor, according to whether losses occur mainly on the *n*- or *p*-side of the junction. The diagrams for Ge and GaAs are represented in Figs 10 and 11, respectively.

For *n*-type Ge (Fig. 10, heavy lines), for a given power (below 10 mw), or a given peak current (below 100 ma), the only way to increase the frequency is to increase the current density; a factor 10 in current density brings a factor 5 in frequency. For a given current density, the highest power-frequency product lies on the harmonic limit ($\lambda = 0.57$), where the frequency is minimum. Any attempt to increase the frequency at constant current density will rapidly lower the power output.

Concerning the other limitations, the diagram of Fig. 10 shows that the higher power requires a prohibitively low characteristic impedance. Even an impedance as low as 1 ohm does not allow for output power larger than 7 mw, and this power is obtained at a frequency of 11 kMc almost exactly at the upper point of the constant current density line $J_p = 10^5$ A/cm². For this reason, this particular point on the power-frequency diagram represents a very favorable combination. Further restrictions are due to the minimum achievable junction diameter, and set a lower limit to the power or an upper limit to the frequency. For example, on the line of constant current density, the point $d_1 = 10$ μm is very close to the maximum power point, so that the above-mentioned point should be considered as also the point of highest frequency. A reduction of the junction diameter or a rise of the current density would increase both frequency and power.

The properties obtained with *p*-type Ge are shown on the same diagram (dashed lines). The slightly higher resistivity of *p*-type materials has the effect of reducing the available output power for a given current density.

The picture changes drastically for *n*-type GaAs (Fig. 11, heavy lines). The combined effect of a larger energy gap and a smaller resistivity displaces the harmonic limit towards much higher powers and the constant current density lines towards higher frequencies. It seems that large improvements are possible. Unfortunately, high powers are not possible without extremely low characteristic impedances, and high frequencies without an extreme reduction of at least one dimension. If the same restrictions as before are considered, the most favorable case is found at the intersection of the line $Z = 1$ ohm with the line $h = 10$ μm, for which the frequency is 27 kMc and the power 3.4 mw. The highest possible frequency with a junction diameter d_1 of 10 μm is only slightly higher, but a reduction of this diameter to 1 μm would allow it to reach the maximum current density of 10^5 A/cm² and a frequency of 140 kMc at a power of 70 μw.

P-type GaAs (dashed lines on the same diagram) has a much higher resistivity and gives results closer to Ge. Current density (10^2 A/cm²) and harmonic limit ($\lambda = 0.57$) are the limiting factors and lead in the best condition to a frequency of 8.2 kMc at a power of 11.5 mw.

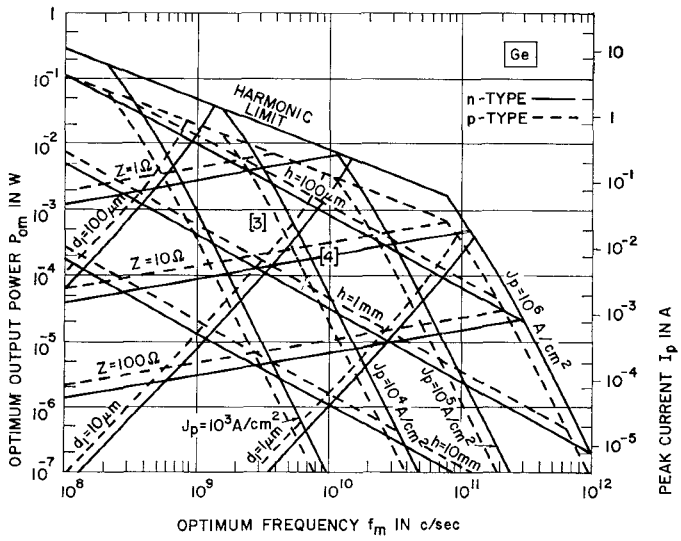

Fig. 10—Power-frequency diagram for Case B, *n*- and *p*-type Ge.

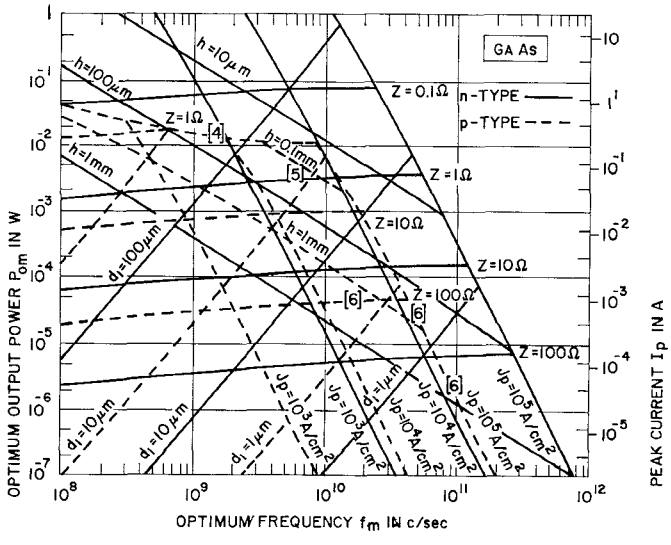

Fig. 11—Power-frequency diagram for Case B, *n*- and *p*-type GaAs.

VI. Conclusion

This analysis showed the order of magnitude of the frequency and power to be expected in a single tunnel diode generator. An optimization on the circuit level indicated how to make the best use of a given device. The influence of the dimensions of a cavity geometry was considered and permitted to relate the performances of the circuit with the bulk and junction properties of the semiconductor. On the basis of empirical data, a correlation between bulk and junction properties was established, which reduced the number of independent variables to one, the peak current density, for a given semiconductor material. Numerical considerations with two idealized cavity geometries were represented on diagrams summarizing the properties of oscillators for n- and p-type Ge and GaAs and typical peak current densities. The first geometry, in which the losses occur in a column having the diameter of the junction and the height of the cavity, restricts the output power to definite levels, but leaves complete freedom regarding upper frequency limit, as far as material only is considered. The second geometry, in which losses are distributed in the bottom of the cavity, presents both frequency and power limitations, with a certain possibility of trading between them. Besides the material, other limiting conditions are set by the smallest practical dimensions and characteristic impedance, which eliminate many possibilities and control the best over-all performances of a generator almost independently of the geometry. It was observed that an output power of 5 mw at a frequency of 30 kMc represents an upper limit in performance of a single tunnel diode generator unlikely to be passed without tremendous practical difficulties.

The results of this analysis are considered as being rather optimistic due to some of the assumptions made at the beginning. In particular, skin effect is likely to reduce the effective current density and to increase losses. The nonlinear junction capacitance reduces the frequency stability and introduces supplementary harmonics which dissipate energy at other than the required frequency. Delay effects in the voltage current characteristics are equivalent to a supplementary series inductance, and reduce the frequency of operation.

The coupling of the power has not been considered here. The small dimensions of the cavity preclude inductive or capacitive coupling used in large size cavities. An ingenious solution, proposed recently by Hauer [5], consists in adjoining a short-circuited half wavelength line. The outside wall of the cavity is replaced by a resistive wall which suppresses an unwanted low-frequency mode and is located at a voltage node for the desired mode.

On the other hand, the optimization procedure consisting in evaluating the maximum of the frequency-power product assumed a complete freedom in the choice of the efficiency and the coupling coefficient. A different procedure should be adopted in presence of each particular limitation, leading possibly to some local improvement of the performance.

Multiple diode generators could be used where higher power levels are required. Some additional difficulties are to be expected from the synchronization, the low impedance power supply and the coupling problems. It seems unlikely that tunnel diode generators will be of any practical interest for power outputs of 1 watt or higher at microwave frequencies.

Acknowledgment

The author wishes to acknowledge the helpful discussions and encouragement of R. F. Rutz during this study.

References

[1] L. Esaki, "New phenomenon in narrow Ge p-n junctions," *Phys. Rev.*, vol. 109, pp. 603–604; January 1958.
[2] E. F. Rutz, "A 3000-Mc lumped-parameter oscillator using an Esaki negative-resistance diode," *IBM J. Res. and Dev.*, vol. 3, pp. 372–374; October, 1959.
[3] F. Sterzer an D. E. Nelson, "Tunnel diode microwave oscillators," Proc. IRE, vol. 49, pp. 744–753; April, 1961.
[4] F. Sterzer, Figure quoted at the 1962 International Solid State Circuits Conference, Phila. in the discussion session on Microwave Power Sources.
[5] W. B. Hauer, "A 4-mw, 6 kMc tunnel-diode oscillator," 1962 Internat'l Solid-State Circuits Conf., *Digest of Technical Papers*, Lewis Winner, New York, N. Y.; p. 68.
[6] C. A. Burrus, "Gallium arsenide Esaki diodes for high frequency applications," *J. Appl. Phys.*, vol. 32, pp. 1031–1036; June, 1961.
[7] G. Dermit, "High frequency power in tunnel diodes," Proc. IRE, vol. 49, pp. 1033–1042; June, 1961.
[8] H. J. Oguey, "Analysis of Tunnel Diode Oscillators," Thomas J. Watson Res. Ctr., Yorktown Heights, N. Y., IBM Res. Rept. RC-504.
[9] B. van der Pol, "The nonlinear theory of electric oscillations," Proc. IRE, vol. 22, pp. 1051–1086; September, 1934.
[10] N. Minorsky, "Introduction to Non-Linear Mechanics," J. W. Edwards Publishers, Inc., Ann Arbor, Mich.; 1947.
[11] E. Fisher, "The period and amplitude of the van der Pol limit cycle," *J. Appl. Phys.*, vol. 25, pp. 273–274; March, 1954.
[12] W. S. Krogdahl, "Numerical solutions of the van der Pol equation," *Z. Angew. Math. Phys.*, vol. 11, pp. 59–63; January, 1960.
[13] W. L. Miranker, "The Occurrence of Limit Cycles in the Equations of a Tunnel Diode Circuit," submitted to IRE Trans. on Circuit Theory.
[14] M. Schuller and W. W. Gartner, "Large-signal circuit theory for negative-resistance diodes, in particular tunnel diodes," Proc. IRE, vol. 49, pp. 1269–1278; August, 1961.
[15] R. Trambarulo, "Some X-band microwave Esaki-diode circuits," 1961 Internat'l Solid-State Circuits Conf., *Digest of Technical Papers*, Lewis Winner, New York, N. Y.; pp. 18–19.
[16] I. A. Lesk, N. Holonyak, U. S. Davidsohn, and N. W. Aarons, "Germanium and silicon tunnel diodes—design, operation and application," 1959 IRE WESCON Convention Record, pt. 3, pp. 9–31.
[17] F. E. Terman, "Radio Engineers Handbook," McGraw-Hill Book Company, Inc., New York, N. Y., p. 58; 1943.
[18] M. E. Hines, "High-frequency negative-resistance circuit principles for Esaki diode applications," *Bell. Sys. Tech. J.*, vol. 39, pp. 477–514; May, 1960.
[19] C. Lanza, and F. H. Dill, private communications.
[20] E. Spenke, "Electronic Semiconductors," McGraw-Hill Book Company, Inc., New York, N. Y., pp. 109–111; 1958.
[21] W. G. Spitzer, F. A. Trumbore, and R. A. Logan, "Properties of heavily doped N-type germanium," *J. Appl. Phys.*, vol. 32, pp. 1822–1830; October, 1961.
T. S. Seidel, "Hall Measurements on Tunnel Diode Materials," *Proc. of the Tech. Conf. on Metallurgy of Elemental and Compound Semiconductors*, Boston, 1960, R. O. Grubel, Ed., vol. 12, pp. 453–463.
[22] C. Hilsum and A. C. Rose-Innes, "Semiconducting III-V Compounds," Pergamon Press, New York, N. Y., p. 140; 1961.
F. D. Rosi, D. Meyerhofer, and R. V. Jensen, "Properties of P-type GaAs prepared by copper diffusion," *J. Appl. Phys.*, vol. 31, pp. 1105–1108; June, 1960.